Journal of Nuclear Medicine, published on December 4, 2020 as doi:10.2967/jnumed.120.243840

Title: Advances in Receptor-Targeted Radiolabeled Peptides for Melanoma Imaging and Therapy

Author: Yubin Miao[1*], Thomas P. Quinn[2, 3,*]

Affiliation: [1]Department of Radiology, School of Medicine, University of Colorado Denver, Aurora, Colorado 80045; [2]Department of Biochemistry, University of Missouri-Columbia, Columbia, Missouri 65211; [3]Harry S. Truman Veterans' Hospital, Columbia, Missouri 65201, USA.

Corresponding Authors:

Yubin Miao, 12700 East 19th Avenue, Department of Radiology, School of Medicine, University of Colorado Denver, Aurora, CO 80045, USA. Phone: 303-724-3763; E-mail: yubin.miao@cuanschutz.edu

Thomas P. Quinn, Department of Biochemistry, University of Missouri-Columbia, 117 Schweitzer Hall, Columbia, MO 65211, USA. Phone: 573-882-6099; E-mail: quinnt@missouri.edu

Running Title: Melanoma imaging and therapy

The Word Count of the Manuscript: 4005

ABSTRACT

Melanocortin-1 receptor (MC1R) and very late antigen-4 (VLA-4, integrin $\alpha_4\beta_1$) are two attractive molecular targets for developing peptide radiopharmaceuticals for melanoma imaging and therapy. MC1R- and VLA-4-targeting peptides and peptide-conjugated Cornell prime dots (C' dots) can serve as delivery vehicles to target both diagnostic and therapeutic radionuclides to melanoma cells for imaging and therapy. This review highlights the advances of MC1R- and VLA-4-targeted radiolabeled peptides and peptide-conjugated C' dots for melanoma imaging and therapy. The promising preclinical and clinical results of these new peptide radiopharmaceuticals present an optimistic outlook for clinical translation into receptor-targeting melanoma imaging and radionuclide therapy in the future.

Keywords: Melanocortin-1 receptor; very late antigen-4; peptide radiopharmaceuticals; Cornell prime dots; melanoma imaging and therapy

INTRODUCTION

Malignant melanoma is the most lethal form of skin cancer.. with approximately 100,350 new cases and 6,850 fatalities in the United States in 2020 (*1*). Metastatic melanoma is extremely aggressive which leads to the high mortality rate of melanoma. The traditional median overall survival of metastatic melanoma patients is less than 9 months. New molecular treatments, such as Vemurafenib (BRAF inhibitor), ipilimumab (targeting CTLA-4) and Nivolumab (PD-1 inhibitor), have improved the overall survival of metastatic melanoma patients by months. However, the treatments are still far from satisfactory because the 5-year survival is approximately 35% for metastatic melanoma patients (*2*). Clearly, there is a great need to develop new theranostic approaches for metastatic melanoma.

Melanin and melanocortin-1 receptor (MC1R) are two attractive molecular targets for melanoma. Melanin is a negatively-charged dark pigment that is produced by melanocytes, and exists in most melanomas and neoplastic melanocytes that ultimately develop to melanoma. MC1R is a G protein-coupled receptor and is over-expressed on mouse and human melanoma cells (*3,4*), as well as on greater than 80% of melanotic and amelanotic human metastatic melanoma samples (*4*). The reports of a melanin-targeting N-(2-(diethylamino)-ethyl)-^{18}F-5-fluoropicolinamide (^{18}F-P3BZA) and a MC1R-targeting ^{68}Ga-DOTA-GGNle-CycMSH$_{hex}$ {DOTA: 1,4,7,10-tetraazacyclononane-1,4,7,10-tetraacetic acid} on melanoma patients (*5,6*) have demonstrated the clinical relevance of both targets for melanoma imaging. Over the past several years, very late antigen-4 (VLA-4, integrin $\alpha_4\beta_1$) has emerged as another attractive molecular target for melanoma due to its expression on melanoma, and the correlation between the expression of VLA-4 integrin and melanoma progression and metastasis (*7-9*).

This review focuses on the preclinical and clinical studies of melanoma using MC1R- and VLA-4-targeted radiolabeled peptides and Cornell prime dots (C' dots) to highlight the advances predominately within the past five years due to its concise feature. Because it takes more than a decade to develop peptides, optimize their pharmacokinetic properties and reach the milestone of clinical translation, several research and review articles published in the last decade are included to present a historic perspective in this review. The promising preclinical and clinical results of new MC1R- and VLA-4-targeted peptide radiopharmaceuticals highlighted in this review present an optimistic outlook for clinical translation into receptor-targeting melanoma imaging and radionuclide therapy in the future.

MC1R-TARGETED DIAGNOSTIC AND THERAPEUTIC α-MELANOCYTE-STIMULATING HORMONE (α-MSH) PEPTIDES

MC1R has been an attractive molecular target for developing peptide radiopharmaceuticals for melanoma imaging and targeted radionuclide therapy. The illustration of MC1R-targeted melanoma imaging using a radiolabeled cyclic α-MSH peptide is presented in Fig. 1. The α-MSH peptide can target diagnostic radionuclides to melanoma cells for imaging and deliver therapeutic radionuclides to melanoma cells for radionuclide therapy. Native α-MSH is a linear peptide with 13 amino acids (Ac-Ser^{1}-Tyr^{2}-Ser^{3}-Met^{4}-Glu^{5}-His^{6}-Phe^{7}-Arg^{8}-Trp^{9}-Gly^{10}-Lys^{11}-Pro^{12}-Val^{13}-NH_2). The moiety of His^{6}-Phe^{7}-Arg^{8}-Trp^{9} is MC1R binding sequence. Since native α-MSH is subject to proteolytic degradation in vivo, non-natural amino acids such as Norleucine^{4} (Nle^{4}) and D-Phe^{7} were introduced to stabilize the bioactive conformation of the peptide, resulting in the discovery of NDP-MSH with sub-nanomolar MC1R binding affinity (*10*). Building on the construct of NDP-MSH, Quinn, Eberle and Cheng groups have reported several radiolabeled linear DOTA-NDP-MSH and DOTA-NAPamide (Ac-Nle-Asp-His-D-Phe-Arg-Trp-Gly-Lys(DOTA)-NH_2) peptides for melanoma imaging, and their promising preclinical results have been summarized by several review articles (*11-14*).

Peptide cyclization with disulfide bond, lactam or site-specific metal has been successfully utilized to enhance MC1R binding and biological activity of cyclic α-MSH peptides. As compared to linear peptides, the cyclic α-MSH peptides possess less conformational flexibility, making them better fit the MC1R binding pocket for improved binding affinities. As shown in Fig. 1, Quinn and colleagues pioneered and developed a novel class of radiolabeled metal-cyclized α-MSH peptides that achieved cyclization and radiolabeling simultaneously when labeled with ^{99m}Tc/^{188}Re. Building on the success of ^{99m}Tc-(Arg^{11})CCMSH (Cys^{3}-Cys^{4}-Glu^{5}-

His^{6}-D-Phe^{7}-Arg^{8}-Trp^{9}-Gly^{10}-Arg^{11}-Pro^{12}-Val^{13}-NH_2), non-radioactive Re was utilized to cyclize the peptide when DOTA was coupled to the peptide for radiolabeling of other theranostic radionuclides including ^{111}In, ^{64}Cu, ^{86}Y,^{177}Lu-, ^{90}Y and ^{212}Pb (*15-17*). Those metal-cyclized α-MSH peptides have demonstrated very promising preclinical results for melanoma imaging and therapy, and have been highlighted by several review articles (*11-14*).

Lactam-cyclized α-MSH peptides have been developed by Santos and Miao groups for radiolabeling of diagnostic radionuclides including ^{99m}Tc, ^{111}In, ^{67}Ga, ^{64}Cu for melanoma imaging over the past years (*18-22*). Santos and colleagues examined the effect of different azolyl-ring substitution patterns of pyrazolyl-diamine bifunctional chelators on the pharmacokinetics of ^{99m}Tc(CO)$_3$-Pz$^{1-4}$-βAlaNle-CycMSH$_{hex}$ {c[Asp-His-D-Phe-Arg-Trp-Lys]-$CONH_2$} (*18*). ^{99m}Tc(CO)$_3$-Pz^{3}-βAlaNle-CycMSH$_{hex}$ exhibited high B16/F1 melanoma uptake (11.82 ± 3.91 %ID/g at 1 h post-injection). The introduction of a carboxylate group in the azolyl-ring resulted in a remarkable reduction of the kidney and liver accumulation.

Miao and colleagues utilized hydrazinonicotinamide (HYNIC)/DOTA/1,4,7-triazacyclononane-1,4,7-triacetic acid (NOTA) for radiolabeling of ^{99m}Tc, ^{111}In, ^{67}Ga and ^{64}Cu, building on the construct of GlyGlyNle-CycMSH$_{hex}$ (*19-22*).The B16/F1 melanoma uptake of these radiolabeled GGNle-CycMSH$_{hex}$ peptides ranges from 12.39 ± 1.61 to 25.53 ± 2.22 %ID/g at 2 h post-injection. Interestingly, the GlyGly linker led to the favorable tumor targeting and urinary clearance for ^{111}In-, ^{67}Ga-, ^{64}Cu-labeled DOTA/NOTA-GGNle-CycMSH$_{hex}$ (*19-21*), whereas the 8-aminooctanoic acid (Aoc) linker resulted in higher tumor uptake of ^{99m}Tc(EDDA)-HYNIC-AocNle-CycMSH$_{hex}$ as compared to ^{99m}Tc(EDDA)-HYNIC-GGNle-CycMSH$_{hex}$ (*22*). To take advantage of the readiness of the $[^{99m}Tc(CO)_3(OH_2)_3]^+$ tricarbonyl kit, they further developed ^{99m}Tc(CO)$_3$-NOTA-GGNle-CycMSH$_{hex}$ (*23*). Interestingly, the switch from HYNIC

to NOTA dramatically increased the melanoma uptake (19.76 ± 3.62 %ID/g at 2 h post-injection) and decreased the renal and liver uptake of $^{99m}Tc(CO)_3$-NOTA-GGNle-CycMSH$_{hex}$ (1.59 ± 0.52 and 1.57 ± 0.32 %ID/g at 2 h post-injection). Importantly, NOTA-GGNle-CycMSH$_{hex}$ could serve as a versatile peptide platform for radiolabeling of ^{99m}Tc, $^{67/68}Ga^{3+}$ and $^{64}Cu^{2+}$ for single photon emission computed tomography (SPECT) and positron emission tomography (PET) imaging of melanoma.

Building upon the success of GGNle-CycMSH$_{hex}$, Bénard and colleagues replaced GlyGly linker with 4-amino-(1-carboxymethyl) piperidine (Pip) and identified ^{68}Ga-DOTA-Pip-Nle-CycMSH$_{hex}$ as a promising conjugate for further evaluation due to its high B16/F10 melanoma uptake (21.9 ± 4.6 %ID/g at 2 h post-injection) (*24*). Furthermore, they used ammoniomethyl-trifluoroborate ($AmBF_3$) moiety to generate ^{18}F-$AmBF_3$-Pip-Nle-CycMSH$_{hex}$ for melanoma imaging. High B16/F10 melanoma uptake (11.96 ± 2.31 %ID/g at 2 h post-injection) and fast urinary clearance of ^{18}F-$AmBF_3$-Pip-Nle-CycMSH$_{hex}$ warranted its further evaluation (*25*).

The persistent translation efforts with HYNIC/DOTA/NOTA-GGNle-CycMSH$_{hex}$ peptides eventually led to the first-in-human study of ^{68}Ga-DOTA-GGNle-CycMSH$_{hex}$ on melanoma patients with metastases (*5*). Gallium-68 is an attractive PET radionuclide which can be readily obtained through a commercial ^{68}Ge/^{68}Ga generator. Miao, Kratochwil and colleagues demonstrated the MC1R-specificity of ^{68}Ga-DOTA-GGNle-CycMSH$_{hex}$ on B16/F10 murine melanoma and M21 xenografted human melanoma (24.27 ± 3.74 and 6.07 ± 0.68 %ID/g at 1 h post-injection, respectively). Then they performed the first-in-human imaging of ^{68}Ga-DOTA-GGNle-CycMSH$_{hex}$ on two melanoma patients with metastases. As shown in Fig. 1, the melanoma metastases in brain, lung, connective tissue, and bulky metastases in small intestine were clearly visualized by ^{68}Ga-DOTA-GGNle-CycMSH$_{hex}$ PET. The remarkable images of

those metastases in patients demonstrated the clinical relevance of MC1R as a valid and attractive molecular target for melanoma imaging, highlighted the potential of ^{68}Ga-DOTA-GGNle-CycMSH$_{hex}$ as a MC1R-targeting probe for human melanoma imaging, and underscored the need for developing MC1R-targeting therapeutic peptides to treat metastatic melanoma patients.

The substitution of diagnostic radionuclides with therapeutic radionuclides (β- and α-emitters) can generate therapeutic α-MSH peptides for melanoma treatment. Miao and colleagues developed and evaluated ^{177}Lu/^{90}Y-DOTA-GGNle-CycMSH$_{hex}$ on B16/F1 and B16/F10 melanoma-bearing mice (*26,27*). Both ^{177}Lu- and ^{90}Y-DOTA-GGNle-CycMSH$_{hex}$ exhibited high MC1R-mediated melanoma uptake (21.63 ± 6.27 and 19.93 ± 5.73 %ID/g at 2 h post-injection) and rapid urinary clearance, warranting further evaluation for melanoma therapy.^{212}Pb is an attractive radionuclide for targeted alpha therapy which can be easily obtained from a ^{224}Ra-^{212}Pb generator. ^{212}Pb decays to ^{212}Bi via a beta-decay (0.57 MeV), then ^{212}Bi eventually decays to stable ^{208}Pb through a branched decay scheme yielding two beta particles (1.8 and 2.2 MeV) and two alpha particles (6.1 and 8.8 MeV). ^{203}Pb/^{212}Pb are attractive matched-pair theranostic radionuclides. The radiolabeling of ^{203}Pb/^{212}Pb can be achieved under identical conditions. Miao and colleagues reported that ^{203}Pb-DOTA-GGNle-CycMSH$_{hex}$ displayed similar MC1R-specific uptake on B16/F1 and B16/F10 melanoma lesions (12.61 ± 2.28 vs. 16.81 ± 5.48 %ID/g at 2 h post-injection) (*28*). The B16/F10 pulmonary metastatic melanoma lesions could be clearly imaged by ^{203}Pb-DOTA-GGNle-CycMSH$_{hex}$ SPECT. The favorable melanoma targeting property of ^{203}Pb-DOTA-GGNle-CycMSH$_{hex}$ warranted the evaluation of ^{212}Pb-DOTA-GGNle-CycMSH$_{hex}$ for melanoma therapy.

MC1R-TARGETED α-MSH-FUNCTIONALIZED DIAGNOSTIC AND THERAPEUTIC CORNELL PRIME DOTS (C' DOTS)

Ultrasmall (< 8 nm dia.) hybrid inorganic core and organic shell nanomaterials are under development for MC1R-targeted multiplexed-image guided surgery, radioimaging and targeted therapy (*29*). Cornell prime dots (C' dots) are near-infrared (NIR) fluorescent silica nanoparticles surface functionalized polyethylene glycol (PEG) with the ability to display biomarker targeting ligands (*30*). cRGDY-PEG-Cy5-C' dots have achieved Investigational New Drug approval and are in Phase 1 and Phase 2 trials for radioimaging and image guided surgery (*31*).

MC1R-avid C' dots were investigated for their potential as melanoma multimodal optical (*32*) and radioimaging agents (*29*) as well as targeted therapeutics (*33,34*). PEG-Cy5-C' dots were surface functionalized with the rhenium (Re)-cyclized α-MSH peptide Ac-Cys-$(Ahx)_2$-D-Lys-Re[Cys^3-Cys^4-Glu^5-His^6-D-Phe^7-Arg^8-Trp^9-Cys^{10}]-Arg^{11}-Pro^{12}-Val^{13}-NH_2 (Fig. 2). Multidentate peptide display yielded particles with an IC_{50} value of 0.66 nM, which was ~10× higher affinity than the targeting DOTA-α-MSH peptide. In vitro cell uptake and competitive binding studies performed with α-MSH-C' dots demonstrated melanoma selective cell binding, internalization and low efflux (*29*).

Biodistribution studies were performed with ^{125}I-labeled α-MSH-PEG-Cy5-C' dots in both M21 human melanoma xenografts and B16/F10 syngenetic mouse models (*29*). Tissue uptake in the individual mouse models varied slightly, but the trends were similar. Favorable pharmacokinetic properties were observed with blood levels at ~15-20 %ID/g at 4 h, ~5-10 %ID/g at 24 h and ~ 1 %ID/g at 72 h. Renal clearance was >100 %ID/g at 1 h and >30 %ID/g at 4 h. Liver and spleen uptake values were low at < 5 %ID/g at 24 h. Maximal tumor uptake of 5-6 %ID/g was observed at 24 h post-injection. PET imaging studies were performed with

^{89}Zr[DFO]-radiolabeled α-MSH-PEG-Cy5-C' dots. ^{89}Zr[DFO]-α-MSH-PEG-Cy5-C' dots PET images showed high tumor to background at 24, 48 and 96 h post-injection that could be blocked by co-injection of the NDP-MSH peptide, demonstrating tumor selectivity. Quantitation of the PET images revealed a tumor uptake of 5.5 ± 0.9 %ID/g with liver uptake values of < 3 %ID/g.

The therapeutic potential of the DOTA-α-MSH-PEG-Cy5-C' dots was examined with the β-emitter ^{177}Lu and the α-emitter ^{225}Ac (*33,34*). The DOTA-α-MSH-PEG-Cy5-C' dots were radiolabeled with ^{177}Lu at >95% radiochemical yield resulting in a specific activity (SA) of 2.035×10^{11} MBq/mol (*33*). Therapy studies were performed in M21 and B16/F10 tumor mice treated with 18.5 MBq ^{177}Lu-DOTA-α-MSH-PEG-Cy5-C' dots, 18.5 MBq ^{177}Lu-DOTA-PEG-Cy5-C' dots, DOTA-α-MSH-PEG-Cy5-C' dots or PBS vehicle control. Statistical analysis of the data demonstrated that mice receiving radiolabeled C' dots had a significant improvement in survival over the non-radiolabeled C' dots and PBS controls. Importantly, there was a significant increase in survival of mice treated with 18.5 MBq ^{177}Lu-DOTA-α-MSH-PEG-Cy5-C' dots compared to non-targeted 18.5 MBq ^{177}Lu-DOTA-PEG-Cy5-C' dots, demonstrating the utility of the MC1R targeting.

Therapy studies with alpha-particle emitting ^{225}Ac-DOTA-α-MSH-PEG-Cy5-C' dots were performed in B16/F10 melanoma tumor bearing mice (*34*). A two-step approach was employed to produce ^{225}Ac-DOTA-α-MSH-PEG-Cy5-C' dots, yielding a SA of 2.361×10^{8} MBq/mol. The therapy study included groups treated with 0.0111 MBq ^{225}Ac-DOTA-α-MSH-PEG-Cy5-C' dots, 0.0111 MBq ^{225}Ac-DOTA-PEG-Cy5-C' dots, and a human serum albumin vehicle control. Kaplin-Meier analysis revealed median survival times of 26, 21, and 14 days post-injection, respectively. A Log-rank test showed that the treatment groups had a statistical improvement in mean survival time and that mice treated with ^{225}Ac-DOTA-α-MSH-PEG-Cy5-C' dots had a

statistically significant survival time over ^{225}Ac-DOTA-PEG-Cy5-C' dots treated mice. An analysis of macrophage, T-cell and NK populations present in the α-irradiated tumor microenvironment revealed dynamic and time-dependent changes, suggesting that combination immunotherapeutic approaches may increase treatment efficacy. Interestingly, the non-radioactive DOTA-PEG-Cy5-C' dots also induced comparable changes in the tumor microenvironment, although their cytotoxicity was much less than the ^{225}Ac-DOTA-PEG-Cy5-C' dots.

VLA-4-TARGETED DIAGNOSTIC AND THERAPEUTIC LLP2A PEPTIDES

VLA-4 is a trans-membrane noncovalent heterodimer that is widely expressed on a variety of tumors such as melanoma, lymphoma, multiple myeloma. The increased expression of the VLA-4 integrin correlates with tumor progression and development of human melanoma metastasis (*7,8*). Lam and colleagues utilized a one-bead-one-compound library to identify a high-affinity peptidomimetic ligand *N*-[[4-[[[(2-ethylphenyl)amino]carbonyl]amino]phenyl]acetyl]-N^{ε}-6-[(*2E*)-1-oxo-3-(3-pyridinyl-2-propenyl)]-L-lysyl-L-2-aminohexanedioyl-(1-amino-1-cyclohexane)carboxamide (LLP2A, IC_{50} = 2 pM) to target VLA-4 (*9*). Building on the construct of LLP2A, DeNardo and colleagues developed and evaluated ^{111}In-labeled DOTA-conjugated LLP2A peptides with or without PEG linkers on Raji lymphoma mouse model. They identified non-PEGylated ^{111}In-DOTA-LLP2A as a lead VLA-4-targeting peptide due to its high tumor to non-tumor uptake ratio for further evaluation (*35*).

Anderson and colleagues conjugated CB-TE1A1P (1,4,8,11-tetraazacyclotetradecane-1-(methane phosphonic acid)-8-(methane carboxylic acid) to LLP2A and evaluated the melanoma targeting property of ^{64}Cu-CB-TE1A1P-LLP2A on B16/F10 melanoma-bearing C57 mice (*36*). Despite higher uptake in VLA-4-rich spleen and bone marrow, the B16/F10 melanoma uptake for ^{64}Cu-CB-TE1A1P-LLP2A was 11.4 ± 2.3 %ID/g at 2 h post-injection. They further conjugated 2-(4,7-bis(carboxymethyl)-1,4,7-triazonan-1-yl)pentanedioic acid (NODAGA) to LLP2A via a polyethylenglycol (PEG_4) linker because NODAGA can form stable complexes with both ^{64}Cu and ^{68}Ga (*37*). The introduction of PEG_4 linker improved the binding affinity of the CB-TE1A1P-LLP2A conjugate by 5-fold. Interestingly, ^{64}Cu-CB-TE1A1P-PEG_4-LLP2A exhibited higher tumor uptake than ^{64}Cu-NODAGA-PEG_4-LLP2A (16.9 ± 2.2 vs. 13.4 ±

1.7 %ID/g at 4 h post-injection), as well as better tumor to non-tumor tissue ratios. Meanwhile, ^{68}Ga-NODAGA-PEG$_4$-LLP2A exhibited lower B16/F10 melanoma uptake than ^{64}Cu-CB-TE1A1P-PEG$_4$-LLP2A. However, melanoma metastases in lung, bone and ovary could be clearly visualized by ^{64}Cu-CB-TE1A1P-PEG$_4$-LLP2A and ^{68}Ga-NODAGA-PEG$_4$-LLP2A (*37*).

^{177}Lu/^{68}Ga-DOTA-PEG$_4$-LLP2A were prepared and evalauted on B16/F10 mleanoma-bearing mice to demonstrate the potential of detecting and treating melanoma (Fig. 3) (*38*). ^{177}Lu-DOTA-PEG$_4$-LLP2A showed very high melanoma uptake of 31.3 ± 7.8 %ID/g at 4 h that significantly decreased to 5.4 ± 1.5 %ID/g at 24 h, although ^{177}Lu-DOTA-PEG$_4$-LLP2A exhibited relatively high uptake in VLA-4-rich spleen, thymus and bone marrow. Meanwhile, ^{68}Ga-DOTA-PEG$_4$-LLP2A displayed 9.1 ± 0.9 %ID/g in B16/F10 tumor at 1 h post-injection. Anderson and colleagues then examined the therapeutic efficay of ^{177}Lu-DOTA-PEG$_4$-LLP2A, alone and combined with immune checkpoint inhibitors (ICIs) (anti-PD-1 + anti-CTLA-4, and anti-PD-L1 + anti-CTLA-4), on B16/F10 melanoma-bearing mice (*39*). ^{177}Lu-DOTA-PEG$_4$-LLP2A treatment (29.97 MBq/mouse) alone exhibited therapeutic efficacy and prolonged the median survival time of control group from 14 d to 19 d, whereas the combination of ^{177}Lu-DOTA-PEG$_4$-LLP2A and ICIs significantly enhanced the median survival time to 22-23 days (Fig. 3) (*39*). The promising therapeutic results warranted further preclinical studies to optimize the combination of therapeutic regimens.

Building upon the promising results of radiometal-labeled LLP2A derivatives, Bénard and colleagues replaced PEG$_4$ linker with PEG$_2$ linker and utilized ^{18}F-AmBF$_3$ to yield DOTA-(^{18}F-AmBF$_3$)-PEG$_2$-LLP2A (*40*). Interestingly, the introduction of DOTA as a hydrophilic moiety increased the B16/F10 tumor uptake of DOTA-(^{18}F-AmBF$_3$)-PEG$_2$-LLP2A to 9.46 ± 2.19 %ID/g and reduced its GI accumulation to 4.55 ± 0.80 %ID/g at 1 h post-injection as compared to ^{18}F-

$AmBF_3$-PEG_2-LLP2A. However, high uptake in VLA-4-positive spleen and bone marrow (28.33 ± 4.28 and 8.23 ± 0.84 %ID/g at 1 h post-injection) may become dose-limiting organs when pursuing the VLA-4-targted therapeutic applications in future studies.

CONCLUSION

Receptor-targeting peptide radiopharmaceuticals continue to receive great interest toward the development of theranostic agents for melanoma. The new MC1R- and VLA-4-targeted radiolabeled peptides and peptide-conjugated C' dots highlighted here represent major advances that will likely have an impact on translational imaging and radionuclide therapy for melanoma in the future. The promising preclinical and clinical results of these new peptide radiopharmaceuticals present an optimistic outlook for clinical translation into receptor-targeting melanoma imaging and radionuclide therapy in the future.

DISCLOSURE

No potential conflict of interest relevant to this article was reported.

ACKNOWLEDGMENTS

The authors appreciated the support from NIH R01CA225837, U54 CA199081-01, P30 CA00874CCSG, University of Missouri peptide synthesis core and Harry Truman Veterans' Hospital Biomolecular Imaging Center and Pharmacology Core.

REFERENCES

1. Siegel RL, Miller KD, Jemal A. Cancer statistics, 2020. *CA Cancer J Clin.* 2020;70:7-30.
2. Weiss SA, Wolchok JD, Sznol M. Immunotherapy of melanoma: facts and hopes. *Clin Cancer Res.* 2019;25:5191-5201.
3. Siegrist W, Solca F, Stutz S, et al. Characterization of receptors for alpha-melanocyte-stimulating hormone on human melanoma cells. *Cancer Res.* 1989;49:6352-6358.
4. Tatro JB, Wen Z, Entwistle ML, et al. Interaction on an α-melanocyte stimulating hormone-diptheria toxin fusion protein with melanotropin receptors in human metastases. *Cancer Res.* 1992;52:2545-2548.
5. Yang J, Xu J, Gonzalez R, Lindner T, Kratochwil C, Miao Y. ^{68}Ga-DOTA-GGNle-CycMSH$_{hex}$ targets the melanocortin-1 receptor for melamoma imaging. *Sci Transl Med.* 2018;10:eaau4445.
6. Ma X, Wang S, Wang S, et al. Biodistribution, radiation dosimetry, and clinical application of a melanin-targeted PET probe, ^{18}F-P3BZA, in patients. *J Nucl Med.* 2019;60:16-22.
7. Schadendorf D, Heidel J, Gawlik C, Suter L, Czarnetzki BM. Association with clinical outcome of expression of VLA-4 in primary cutaneous malignant melanoma as well as P-selectin and E-selectin on intratumoral vessels. *J Natl Cancer Inst*. 1995;87:366–371.
8. Kuphal S, Bauer R, Bosserhoff AK. Integrin signaling in malignant melanoma. *Cancer Metastasis Rev*. 2005;24:195-222.
9. Peng L, Liu R, Marik J, Wang X, Takada Y, Lam KS. Combinatorial chemistry identifies high-affinity peptidomimetics against $\alpha_4\beta_1$ integrin for in vivo tumor imaging. *Nat Chem Biol*. 2006;2:381-389.

10. Sawyer TK, Sanfilippo PJ, Hruby VJ, et al. 4-Norleucine, 7-D-phenylalanine-alpha-melanocyte-stimulating hormone: a highly potent alpha-melanotropin with ultralong biological activity. *Proc Natl Acad Sci USA*. 1980;77:5754-5758.
11. Miao Y, Quinn TP. Alpha-melanocyte stimulating hormone peptide-targeted melanoma imaging. *Front Biosci.* 2007;12:4514-4524.
12. Eberle AN, Rout B, Qi MB, Bigliardi PL. Synthetic peptide drugs for targeting skin Cancer: malignant melanoma and melanotic lesions. *Curr Med Chem*. 2017;24:1797-1826.
13. Miao Y, Quinn TP. Peptide-targeted radionuclide therapy for melanoma. *Crit Rev Oncol Hematol.* 2008;67:213-228.
14. Quinn TP, Zhang X, Miao Y. Targeted melanoma imaging and therapy with radiolabeled alpha-melanocyte stimulating hormone peptide analogues. *Gital Dermatol Venereol.* 2010;145:245-258.
15. Miao Y, Benwell K, Quinn TP. ^{99m}Tc and ^{111}In labeled alpha-melanocyte stimulating hormone peptides as imaging probes for primary and pulmonary metastatic melanoma detection. *J Nucl Med.* 2007;48:73-80.
16. McQuade P, Miao Y, Yoo J, Quinn TP, Welch MJ, Lewis JS. Imaging of melanoma using ^{64}Cu and ^{86}Y-DOTA-ReCCMSH(Arg^{11}), a cyclized peptide analogue of α-MSH. *J Med Chem.* 2005;48:2985-2992.
17. Miao Y, Hylarides M, Fisher DR, et al. Melanoma therapy via peptide-targeted α-radiation. *Clin Cancer Res.* 2005;11:616- 5621.
18. Morais M, Oliveira BL, Correia JD, et al. Influence of the bifunctional chelator on the pharmacokinetic properties of ^{99m}Tc(CO)$_3$-labeled cyclic α-melanocyte stimulating hormone analog. *J Med Chem*. 2013;56:1961-1973.

19. Guo H, Yang J, Gallazzi F, Miao Y. Effects of the amino acid linkers on the melanoma-targeting and pharmacokinetic properties of ^{111}In-labeled lactam bridge-cyclized α-MSH peptides. *J Nucl Med.* 2011;52: 608-616.
20. Guo H, Gallazzi F, Miao Y. Ga-67-labeled lactam bridge-cyclized alpha-MSH peptides with enhanced melanoma uptake and reduced renal uptake. *Bioconjug Chem.* 2012;23:1341-1348.
21. Guo H, Miao Y. Cu-64-labeled lactam bridge-cyclized alpha-MSH peptides for PET imaging of melanoma. *Mol Pharm.* 2012;9:2322-2330.
22. Guo H, Miao Y. Introduction of an aminooctanoic acid linker enhances uptake of Tc-99m-labeled lactam bridge-cyclized alpha-MSH peptide in melanoma. *J Nucl Med.* 2014;55:2057-2063.
23. Qiao Z, Xu J, Gonzalez R, Miao Y. Novel [^{99m}Tc]-tricarbonyl-NOTA-conjugated lactam-cyclized alpha-MSH peptide with enhanced melanoma uptake and reduced renal uptake. *Mol Pharm.* 2020;17:3581-3588.
24. Zhang C, Zhang Z, Lin KS, et al. Preclinical melanoma imaging with ^{68}Ga-labeled α-melanocyte-stimulating hormone derivatives using PET. *Theranostics*. 2017;7:805-813.
25. Zhang C, Zhang Z, Lin KS, et al. Melanoma imaging using ^{18}F-labeled α-melanocyte-stimulating hormone derivatives with positron emission tomography. *Mol Pharm*. 2018;15:2116-2122.
26. Guo H, Miao Y. Melanoma targeting property of a Lu-177-labeled lactam bridge-cyclized alpha-MSH peptide. *Bioorg Med Chem Lett.* 2013;23:2319-2323.
27. Xu J, Yang J, Gonzalez R, Fisher DR, Miao Y. Melanoma-targeting property of Y-90-labeled lactam-cyclized alpha-melanocyte-stimulating hormone peptide. *Cancer Biother Radiopharm.* 2019;*34*:597-603.

28. Yang J, Xu J, Cheuy L, Gonzalez R, Fisher DR, Miao Y. Evaluation of a novel Pb-203-labeled lactam-cyclized alpha-melanocyte-stimulating hormone peptide for melanoma targeting. *Mol Pharm*. 2019;16:1694-1702.
29. Chen F, Zhang X, Ma K, et al. Melanocortin-1 receptor-targeting ultrasmall silica nanoparticles for dual-modality human melanoma imaging. *ACS Appl Mater Interfaces*. 2018;10:4379-4393.
30. Ma K, Mendoza C, Hanson M, Werner-Zwanziger U, Zwanziger J, Weisener U. Control of ultrasmall sub-10 nm ligand-functionalized fluorescent core-shell silica nanoparticle growth in water. *Chem Mater*. 2015;27:4119-4133.
31. Phillips E, Penate-Medina O, Zanzonico PB, et al. Clinical translation of an ultrasmall inorganic optical-PET imaging nanoparticle probe. *Sci Transl Med*. 2014;6:260ra149.
32. Chen F, Madajewski B, Ma K, et al. Molecular phenotyping and image-guided surgical treatment of melanoma using spectrally distinct ultrasmall core-shell silica nanoparticles. *Sci Adv*. 2019;5:eaax5208.
33. Zhang X, Chen F, Turker MZ, et al. Targeted melanoma radiotherapy using ultrasmall ^{177}Lu-labeled α-melanocyte stimulating hormone-functionalized core-shell silica nanoparticles. *Biomaterials*. 2020;241:119858.
34. Urbanska AM, Khanin R, Alidori S, et al. A genomic profile of local immunity in the melanoma microenvironment following treatment with α particle-emitting ultrasmall silica nanoparticles. *Cancer Biother Radiopharm*. 2020;35:459-473.
35. DeNardo SJ, Liu R, Albrecht H, et al. ^{111}In-LLP2A-DOTA polyethylene glycol–targeting $\alpha_4\beta_1$ integrin: comparative pharmacokinetics for imaging and therapy of lymphoid malignancies. *J Nucl Med*. 2009;50:625-634.

36. Jiang M, Ferdani R, Shokeen M, Anderson CJ. Comparison of two cross-bridged macrocyclic chelators for the evaluation of ^{64}Cu-labeled-LLP2A, a peptidomimetic ligand targeting VLA-4-positive tumors. *Nucl Med Biol*. 2013;40:245-251.

37. Beaino W, Anderson CJ. PET imaging of very late antigen-4 in melanoma: comparison of ^{68}Ga- and ^{64}Cu-labeled NODAGA and CB-TE1A1P-LLP2A conjugates. *J Nucl Med*. 2014;55:1856-1863.

38. Beaino W, Nedrow JR, Anderson CJ. Evaluation of ^{68}Ga- and ^{177}Lu-DOTA-PEG$_4$-LLP2A for VLA-4-targeted PET imaging and treatment of metastatic melanoma. *Mol Pharm*. 2015;12:1929-1938.

39. Choi J, Beaino W, Fecek RJ, et al. Combined VLA-4-targeted radionuclide therapy and immunotherapy in a mouse model of melanoma. *J Nucl Med*. 2018;59:1843-1849.

40. Roxin Á, Zhang C, Huh S, et al. A metal-free DOTA-conjugated ^{18}F-labeled radiotracer: [^{18}F]DOTA-AMBF$_3$-LLP2A for imaging VLA-4 over-expression in murine melanoma with improved tumor uptake and greatly enhanced renal clearance. *Bioconjug Chem*. 2019;30:1210-1219.

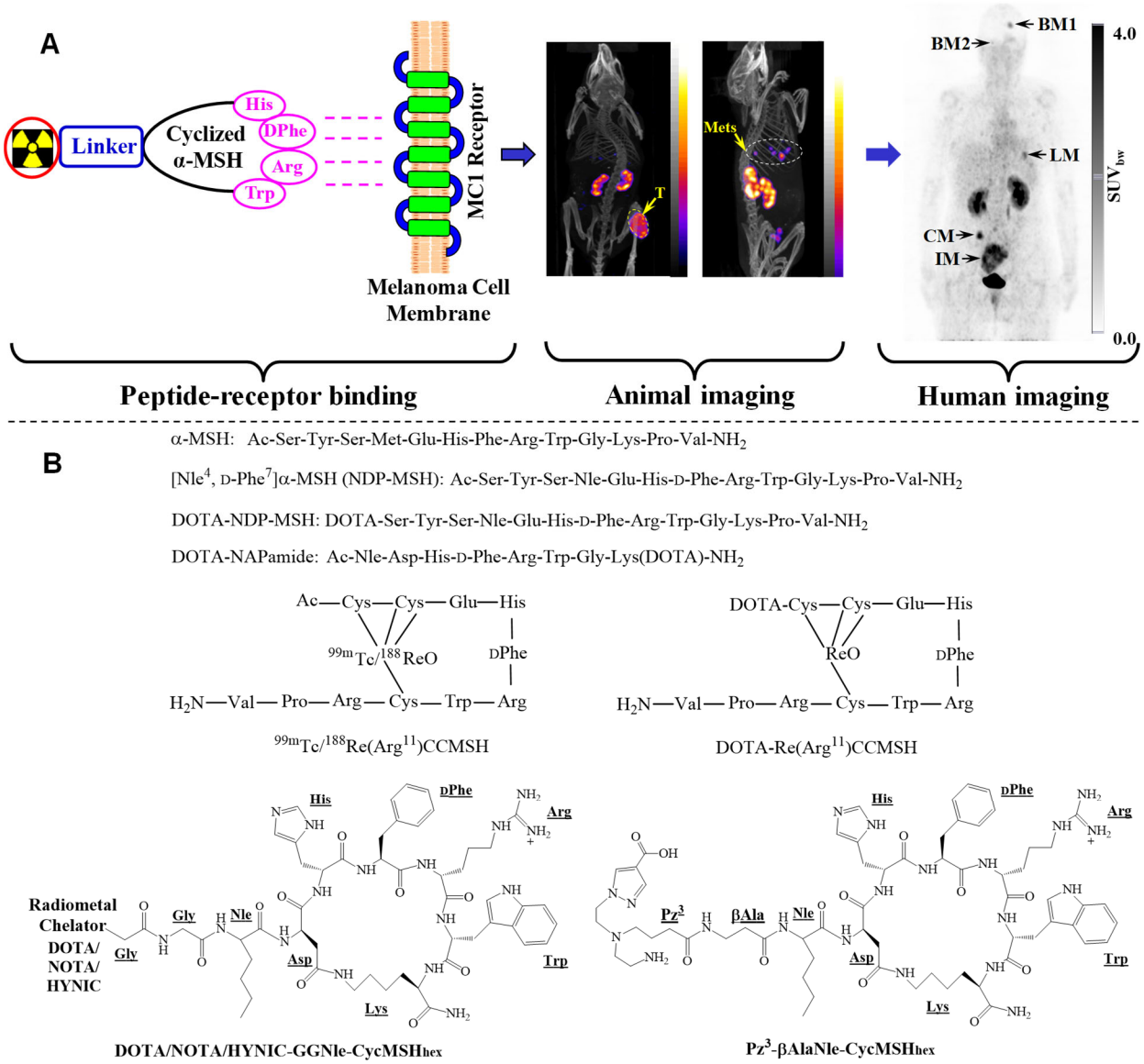

Figure 1. A. Schematic illustration of a MC1R avid radiolabeled α-MSH peptide to detect B16/F1 flank melanoma (T) and B16/F10 pulmonary metastatic melanoma (Mets) in mice and melanoma metastases in a melanoma patient. BM, LM, CM and IM represent melanoma metastases in brain, lung, connective tissue and intestines. B. Representative α-MSH peptides. Human and animal images were reproduced from references 5, 19, 20 by permissions from the American Association for the Advancement of Science, Society of Nuclear Medicine and Molecular Imaging and American Chemistry Society.

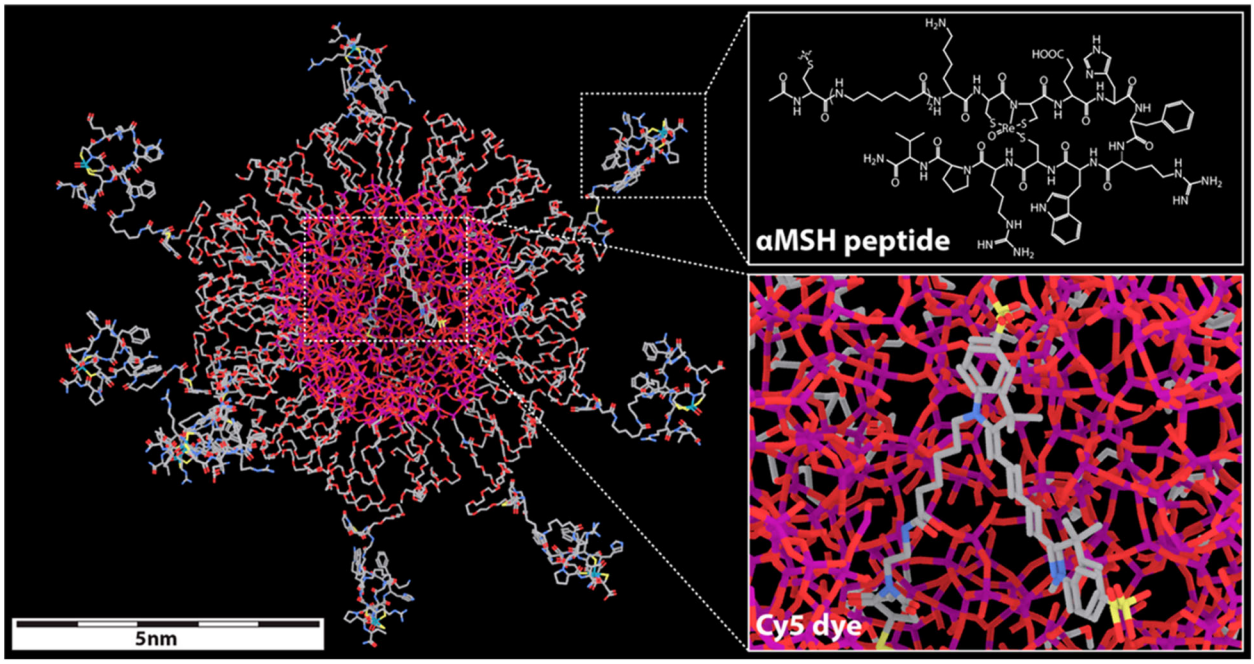

Figure 2. Molecular model of the α-MSH-PEG-Cy5-C' dot. The silicon, oxygen, carbon, nitrogen and sulfur atoms are colored purple, red, gray, blue and yellow, respectively. The DOTA chelator was attached to the epsilon amine of the D-Lys residue for ^{177}Lu and ^{225}Ac radiolabeling. The figure was reproduced from reference 29 by permission from the American Chemistry Society.

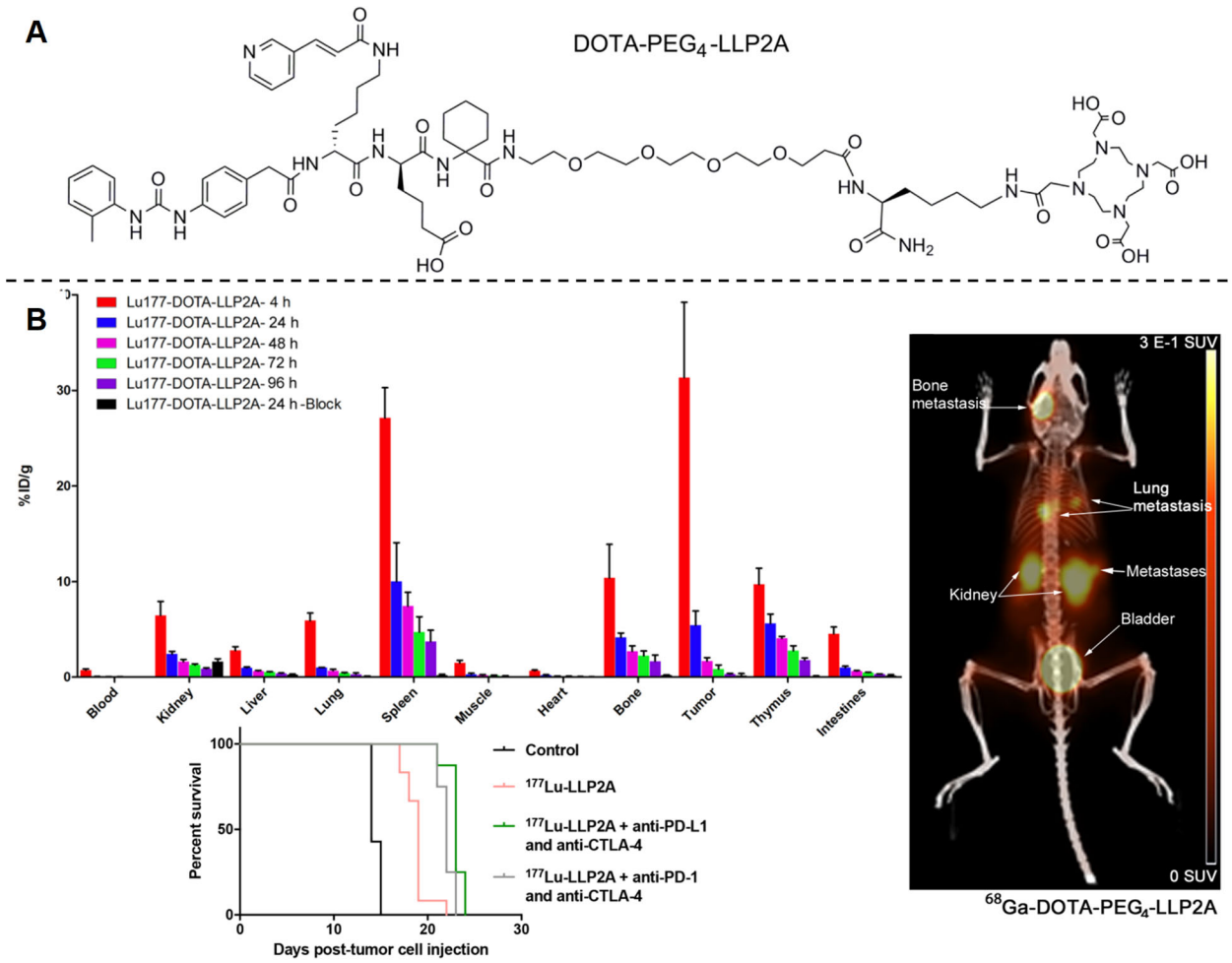

Figure 3. A. Schematic structure of DOTA-PEG$_4$-LLP2A. B. Biodistribution of ^{177}Lu/^{68}Ga-DOTA-PEG$_4$-LLP2A and survival curves of treatments of ^{177}Lu-DOTA-PEG$_4$-LLP2A alone and combined with immune checkpoint inhibitors. The figure was reproduced from references 38 and 39 by permissions from the American Chemistry Society and Society of Nuclear Medicine and Molecular Imaging.